Accepted Manuscript

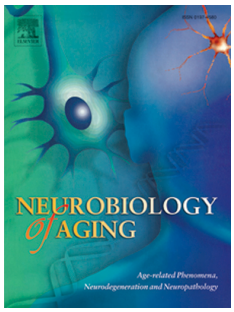

Task-evoked fMRI Changes in Attention Networks are Associated with Preclinical Alzheimer Disease Biomarkers

Brian A. Gordon, PhD, Jeffrey M. Zacks, PhD, Tyler Blazey, BS, Tammie L.S. Benzinger, MD, PhD, John C. Morris, MD, Anne M. Fagan, PhD, David M. Holtzman, MD, David A. Balota, PhD

PII: S0197-4580(15)00052-4

DOI: 10.1016/j.neurobiolaging.2015.01.019

Reference: NBA 9199

To appear in: *Neurobiology of Aging*

Received Date: 14 November 2014

Revised Date: 21 January 2015

Accepted Date: 23 January 2015

Please cite this article as: Gordon, B.A., Zacks, J.M., Blazey, T., Benzinger, T.L.S., Morris, J.C., Fagan, A.M., Holtzman, D.M., Balota, D.A., Task-evoked fMRI Changes in Attention Networks are Associated with Preclinical Alzheimer Disease Biomarkers, *Neurobiology of Aging* (2015), doi: 10.1016/j.neurobiolaging.2015.01.019.

Task-evoked fMRI Changes in Attention Networks are Associated with Preclinical Alzheimer Disease Biomarkers

Brian A Gordon[ab*] PhD, Jeffrey M Zacks[a,c], PhD, Tyler Blazey[d], BS, Tammie LS Benzinger[a,b,d,e], MD, PhD, John C Morris[b,f], MD, Anne M Fagan[b,f,g], PhD, David M Holtzman[b,d,f, g], MD, David A Balota[b,c], PhD

[a] Department of Radiology
[b] Knight Alzheimer's Disease Research Center
[c] Department of Psychology
[d] Division of Biology and Biomedical Sciences
[e] Department of Neurological Surgery
[f] Department of Neurology
[g]The Hope Center for Neurodegenerative Disorders
Washington University in St. Louis

*Dr. Brian A. Gordon
bagordon@wustl.edu
660 South Euclid Ave
Campus Box 8225
St. Louis, MO 63110

Dr. Jeffrey M Zacks	jzacks@wustl.edu
Mr. Tyler Blazey:	blazeyt@mir.wustl.edu
Dr. Tammie LS Benzinger:	benzingert@mir.wustl.edu
Dr. John C Morris	morrisj@abraxas.wustl.edu
Dr. Anne M Fagan	fagana@neuro.wustl.edu
Dr. David M Holtzman	holtzman@wustl.edu
Dr. David A Balota	dbalota@wustl.edu

Highlights

- Functional MRI signatures of attentional control were examined in older adults
- Individuals had varying levels of Alzheimer Disease-related biomarkers
- Task manipulations produced robust block and trial level BOLD signal modulations
- Elevated tau and ptau were associated with an over-activation of attention networks
- Suggests altered attentional control with elevated Alzheimer Disease pathology

Abstract

There is a growing emphasis on examining preclinical levels of Alzheimer Disease-related pathology in the absence of cognitive impairment. Prior work examining biomarkers has focused almost exclusively on memory, although there is mounting evidence that attention also declines early in disease progression. In the current experiment, two attentional control tasks were used to examine alterations in task-evoked functional magnetic resonance imaging (fMRI) data related to biomarkers of Alzheimer pathology. Seventy-one cognitively normal individuals (females=44, mean age=63.5) performed two attention-demanding cognitive tasks in a design that modeled both trial-level and task-level fMRI changes. Biomarkers included $A\beta_{42}$, tau, and phosphorylated tau (ptau) measured from cerebrospinal fluid (CSF), and positron emission tomography (PET) measures of amyloid deposition. Both tasks elicited widespread patterns of activation and deactivation associated with large task-level manipulations of attention. Importantly, results from both tasks indicated that higher levels of tau and ptau pathology were associated with block level over-activations of attentional control areas. This suggests early alteration in attentional control with rising levels of Alzheimer Disease pathology.

Keywords: Alzheimer; attention; biomarkers; fMRI; dementia; amyloid; Alzheimer's; tau; ptau

1. Introduction

Alzheimer disease (AD) is not a static disorder; there is accumulating evidence that pathological processes begin up to twenty years before symptomatic stages (Bateman et al., 2012; Benzinger et al., 2013; Jack et al., 2013). Elevated amyloid (Aβ) deposition in the brain is linked to a rise in hyperphosphorylated forms of tau in neuropil threads and neurofibrillary tangles (NFTs)(Hardy and Higgins, 1992). Aggregated tau leads to neuronal dysfunction and death that manifest *in vivo* as hypometabolism, atrophy, functional abnormalities, and progressive cognitive impairment (Bateman et al., 2012; Jack et al., 2013). The early detection of structural or functional changes in the absence of significant cognitive impairment provides candidate biomarkers and therapeutic targets.

In prior work in the literature, at-risk populations have been identified using genetic markers, such as the ε4 allele of the apolipoprotein (APOE) gene, or high levels of amyloid deposition as evidenced by PET. The majority of fMRI studies examining such populations have used variations of memory encoding tasks (Bondi et al., 2005; Bookheimer et al., 2000; Dennis et al., 2010; Filbey et al., 2010; Han et al., 2007; Mormino et al., 2012; Trivedi et al., 2006). Although failing episodic memory is a hallmark of AD, the disorder is also characterized by attentional impairments (Bäckman et al., 2005; Balota and Faust, 2001; Perry and Hodges, 1999). Attentional control discriminates healthy individuals from those with dementia (Bäckman et al., 2005; Hutchison et al., 2010), predicts progression to dementia in a healthy sample (Balota et al., 2010), and from mild to more severe cognitive impairment (Albert et al., 2001; Sarazin et al., 2007). Early memory deficits in AD may in part be due to an inability to properly allocate attention, rather than pure declines of memory subsystems (Balota and Faust, 2001; Hutchison et

al., 2010). The putative relationship between attention and memory is well-established in the literature (e.g. Craik and Lockhart, 1972; Jacoby, 1991).

Cholinesterase inhibitors used to treat early symptoms of AD prevent the breakdown of acetylcholine (Birks, 2006; Kaduszkiewicz et al., 2005), which is a neurotransmitter heavily implicated in attentional control (Himmelheber et al., 2000; Sahakian et al., 1989; Sarter and Bruno, 1997). The basal forebrain cholinergic system projects to higher cortical areas including anterior cingulate, frontal, and parietal cortex (Selden et al., 1998). These three regions have been repeatedly implicated in neuroimaging studies of attention (Corbetta and Shulman, 2002; Coull and Nobre, 1998; Pardo et al., 1991; Wager et al., 2004). If attentional control is altered in preclinical AD, functional activity in these regions should be sensitive to rising levels of AD pathology.

To better understand the effects of increasing levels of AD pathology in clinically normal populations, we used two well-studied task-evoked fMRI paradigms (Animacy Judgments and Stroop) to examine cognitively normal adults with varying levels of pathology. Sustained attention was manipulated through the alteration between short rest blocks and longer task blocks. An event-related design within each block allowed for the examination of trial specific effects. Biomarkers were quantified using ^{11}[C]Pittsburgh Compound B (PiB) positron emission tomography (PET) and cerebrospinal fluid (CSF) assays. Focusing on attentional control, and including CSF biomarkers, in a task-evoked design provides a novel approach to examining the early influence of AD pathology.

2. Methods

2.1 Study Population

Participants were part of the Adult Children Study at the Knight Alzheimer's Disease Research Center (ADRC) at Washington University in St. Louis. The Adult Children Study is an ongoing project designed to look at cognitively normal individuals with an elevated risk of developing AD. Participants underwent a clinical assessment, neuropsychological assessment, PiB PET imaging, lumbar puncture (LP), structural MRI, and a functional MRI session. Participants were right-handed and cognitively normal (Clinical Dementia Rating, CDR=0) (Morris, 1993). An initial sample of 92 participants was screened down to 79 by excluding individuals with neurological damage (e.g. stroke, traumatic brain injury n=5), a lag between biomarker and MR acquisition (n=5) more than 3 SD from the initial group mean, or a biomarker values (n=3) more than 3 SD from the initial group mean. After screening for motion and abnormal behavior (see details below) the final cohort consisted of 71 individuals. In this final group the mean lag between functional MRI and biomarker assessment was 39 days (median 0, range 0 to 415) for PET and 473 days (median 161, range 1 to 2227) for LPs. Population demographics are presented in Table 1.

2.2. CSF Samples

CSF (20-30 mL) was collected by LP after overnight fasting (Fagan et al., 2006). Total tau, $ptau_{181}$, and $A\beta_{42}$ were measured using ELISA (INNOTEST; Fujirebio, formerly Innogenetics, Ghent, Belgium). The cohort had a mean $A\beta_{42}$ of 770.4 pg/ml (median 779.0, range 285.3-1360.5), mean tau of 250.4 pg/ml (median 225.7, range 100-588.3), and mean $ptau_{181}$ of

53.5 pg/ml (median 48.5, range 24.8-127.2). For descriptive purposes the percent of the population that would be deemed biomarker positive using previous published cutoffs of less than 459 pg/mL for $A\beta_{42}$, greater than 339 pg/mL for tau, and greater than 67 pg/ML for ptau (Vos et al., 2013) is presented in Table 1. Because the distribution of biomarker values had both high levels of skewness and kurtosis, all analyses of CSF values were log transformed to provide a more normal distribution.

2.3 PET Imaging

Methods have been described in detail elsewhere (Su et al., 2013). Participants underwent a 60-minute dynamic scan with PiB. In each region a tissue mask (grey, white, CSF) was generated based upon the FreeSurfer segmentation (Fischl, 2004) (http://freesurfer.net/). A CSF dilution factor was calculated for each region, and the raw time-activity curve for that region was corrected by this dilution factor before its binding potential was calculated. From the dynamic scan binding potentials were calculated using Logan graphical analysis and a cerebellar reference region. An average across both left and right lateral orbitofrontal, inferior parietal, precuneus, rostral middle frontal, superior frontal, superior temporal, and middle temporal regions derived from FreeSurfer was used to create a mean cortical binding potential (MCBP), with a mean value of .29 (median .13, range .02-1.32). Using a previously published approach using a receiver operator curve (Vos et al., 2013), amyloid positivity was determined by comparing a large population (n=212) of cognitive normal individuals against a population of mildly demented (CDR=0.5, n=140) with a confirmed diagnosis of DAT. Using this approach positivity was determined as a MCBP greater than .23. For descriptive purposes the percent of the population that would be deemed biomarker positive is presented in Table 1. As with the CSF biomarkers,

analyses values were log transformed to yield a more normal distribution.

2.4 Task Designs

The task design is depicted in Figure 1. Participants had brief practice with the tasks immediately prior to scanning. In the scanner, participants performed two runs of an animacy judgment task followed by two runs of a Stroop (Stroop, 1935) task. The four runs took a total of 39 minutes and 52 seconds. Both tasks were constructed with similar properties. During each run tasks alternated between 30 seconds of rest and longer task blocks (114-seconds in the Animacy task and 110-seconds in the Stroop task). During rest intervals participants saw a red fixation-cross; during task blocks stimuli were presented above a white fixation-cross. Within each run there were five rest and four task blocks. Each task block consisted of 24 trials equally distributed across trial types (e.g. living/nonliving). Each trial was presented on the screen for 1 second followed by an inter-trial interval of 1, 3, 5, or 9 seconds. Distributions of jitters were skewed such that short intervals were overrepresented. Within a block, presentation order was random, and jitters were counterbalanced across trial types.

The first task required a living/nonliving animacy judgment to words (e.g. horse or diamond). Two lists were created, each consisting of 96 living and 96 nonliving words. Lists were counterbalanced across individuals. Lists were balanced for word length, orthographic neighborhood, and word frequency. Words within a list varied from high (e.g., horse) to low (e.g., locust) word frequency. The second task was a Stroop paradigm, where participants responded whether a word was presented in a blue or red font. The words could be congruent with (e.g., red in red), incongruent with (e.g., blue in red), or contain no color information (e.g., deep in red).

Immediately after scanning, participants completed a surprise memory test outside the scanner. Individuals indicated whether a word had been seen during the Animacy task or whether it was new. They then rated the confidence of their decision from 1 (low) to 5 (high). Participants practiced the judgment procedure using eight words from the practice and eight unseen foils. They then saw 384 words, half of which were new. Trial presentations were self-paced by the participants. In the scanner the Animacy task was always performed before the Stroop Task to maintain a consistent duration between encoding and test. Based upon abnormal behavior (e.g., more than 50 timeouts or severe problems with vocabulary) five individuals were excluded from the analyses of the Animacy task and two from the Stroop Task.

2.5 Scanning Protocol

Data were acquired on a Siemens Trio 3T scanner. T_1-weighted images were acquired using a MPRAGE sequence with: repetition time (TR)=2400 ms, echo time (TE) = 3.16 ms, flip angle (FA) = 8°, field of view (FOV) = 256 mm, in plane resolution 176 x 256, slice thickness = 1mm acquired in sagittal orientation. Images had a 1 mm isotropic resolution.

BOLD data were acquired using a T_2*-weighted gradient-echo interleaved EPI sequence with: TR=2000 ms, TE = 25 ms, FA = 90°, FOV = 256 mm, in plane resolution of 64 x 64, slice thickness= 4mm. 36 sagittal slices were acquired parallel to the anterior-posterior commissural line. Images had a 4 mm isotropic resolution. Each Animacy run lasted for 606 seconds. Each Stroop run lasted for 590 seconds.

2.6 Functional Analyses

A population-specific structural atlas was generated using one hundred older adults drawn from a similar but non-overlapping population as those in the study (CDR=0, age range 46-95, mean=71.3, median 71.0, female n=61) who took part in neuroimaging studies at the Knight ADRC. These images underwent a rigid registration to the MNI152 template. The resulting images were averaged together to produce an initial template. Using this template a further nine-step iterative procedure was used, with the resulting image becoming the target template for the next iteration. This process used two rigid registrations, three affine registrations, and four non-linear registrations with FNIRT (Jenkinson et al., 2012). The final template better represented areas with age related atrophy.

Analyses of the task data were carried out using FEAT, part of FSL (Jenkinson et al., 2012) (www.fmrib.ox.ac.uk/fsl). Preprocessing included correcting for field inhomogeneities, motion correction, high-pass temporal filtering with a cutoff of 150 seconds, and spatial smoothing with a 5 mm FWHM Gaussian kernel. EPIs were aligned to a T_1 image using a boundary based registration procedure and aligned into template space using non-linear warping. Motion parameters were examined for each run. Individuals with an average absolute movement above 1.50 mm, or an average relative movement of .5 mm were excluded from analyses. Using these criteria, a further 8 individuals were excluded from the Animacy analyses and 13 from the Stroop analyses. Combined with the exclusions above, this resulted in 71 unique participants with 66 in the Animacy task and 64 in the Stroop task

For each run, block effects were modeled as a boxcar design convolved with a double-gamma hemodynamic response function. Event-related designs were modeled as events with one-second durations convolved with a double-gamma hemodynamic response function. Runs

within a subject were combined using a fixed-effects model. For each Animacy run two event-related models were computed. The first classified each trial based upon animate or inanimate group membership while simultaneously modeling word frequency as a continuous measure. The second model compared trials that would later be remembered with high confidence to all those later forgotten. For the Stroop task, trial level analyses examined the effects of word and color compatibility.

The combined first level runs for each subject were entered into a higher-level analysis with participant as a random effect using FLAME (Woolrich et al., 2004). For each design (e.g., blocked Stroop effects) the group average was modeled while also including age, gender, and years of education as covariates. Expanded analyses targeted the additional influence of each biomarker. These analyses controlled for the interval between biomarker and MRI assessments by including it as a covariate. For all group level analyses the resulting statistics were corrected for multiple comparisons using a cluster thresholding technique (Worsley et al., 1992) with a z-statistic threshold of 2.3 and cluster probability threshold of $p < 0.05$.

3. Behavioral Results

The behavioral results obtained during both the functional Animacy and Stroop tasks are presented in Table 2. Values represent marginal means controlling for the effects of age, gender, and education. When performing statistical analyses, reaction time (RT) data were z-transformed within each individual to control for scaling differences in individual response latencies (Faust et al., 1999). Due to ceiling effects in the Animacy and Stroop tasks, analyses used Fisher transformed accuracy data rather than raw values. When examining the influences of AD

biomarkers, models included the interval between biomarker and MRI assessments as a covariate. Full results of all models examining the effects of biomarkers are presented in Table 3.

3.1 Animacy Task

Accuracy and RT data obtained during the Animacy task were each modeled using a two (animate/inanimate) by two (high/low frequency) repeated measures analyses. All tests used Wilks' Lambda to assess significance. Participants responded faster ($F_{1,62}$=139.8, p<.0001, η_p^2 = .69) but less accurately ($F_{1,62}$=5.5, p<.05, η_p^2 = .08) to animate words, and they were faster ($F_{1,62}$=257.1, p<.0001, η_p^2 = .81) and more accurate to high frequency words ($F_{1,62}$=41.3, p<.0001, η_p^2 = .40). There were significant animacy by frequency interactions for both RT ($F_{1,62}$=9.5, p <.005, η_p^2 = .13) and accuracy ($F_{1,62}$=7.7, p<.05, η_p^2 = .11), such that the performance cost for low frequency words was larger for animate than inanimate items. For each main analysis additional models were constructed to examine main effects of or interactions with the biomarkers. There were no main effects or interactions with any biomarkers (see Table 3).

3.2 Memory Effects

Behavioral data from the subsequent memory test are shown in Tables 2 and 3. On the memory tests participants were faster, more accurate, and more confident for low frequency words compared to high frequency words. Animate objects were more likely to be judged old, whereas inanimate objects were more likely to be judged new, and the response times were consistent with this pattern (see Supplementary Tables 1 and 2). For ease of interpretation, all further analyses collapsed across trial types.

When examining RT and confidence we fit a two (old/new) by two (correct/incorrect) repeated measures analyses. Participants responded faster to previously seen words ($F_{1,62}$=36.34, p<.0001), were faster on accurate relative to inaccurate trials ($F_{1,62}$=110.44, <.0001), and the effect of accuracy on RT was greater for old relative to new words ($F_{1,62}$=27.14, p<.0001). Participants rated old judgments with higher confidence than new responses ($F_{1,62}$=75.40, p<.0001), rated correct trials higher than incorrect trials ($F_{1,62}$=199.65, p<.0001), and the effect of accuracy was greater for old judgments ($F_{1,62}$=61.30, p<.0001).

For RT, there was a significant exposure (old/new) by biomarker interaction for both tau ($F_{1,60}$=7.03, p<.05) and ptau ($F_{1,60}$=7.18, p<.01) as well as exposure (old/new) by accuracy (correct/incorrect) by biomarker level three-way interaction for tau ($F_{1,60}$=6.58, p<.05) and ptau tau ($F_{1,60}$=6.75, p<.05). After correction for multiple comparisons the three-way interaction with tau fell slightly below significance. The relationships were such that AD biomarker levels had no influence on RT for previously seen trials, but higher levels of tau/ptau were correlated with longer RTs on trials successfully identified as new and with shorter RTs on trials inaccurately identified as old. Thus, the level of AD pathology was related to the response latencies on lure trials, reflected by slowing of the correct rejections but speeding on the false alarms.

3.3 Stroop Task

Accuracy and RT data obtained from the Stroop task were both modeled as repeated measures analyses with three levels (congruent, neutral, and incongruent). There was a significant effect on accuracy ($F_{2,59}$=21.51, p<.0001, η_p^2 = .32) with significant pairwise differences between incongruent and both congruent (t=6.82, p<.0001) and neutral trials (t=5.13, p<.0001), but no difference between congruent and neutral trials (t=2.15, p=.12). There was a

main effect of congruency when examining the reaction time data ($F_{2,59}$=179.57, p<.0001, η_p^2 = .86) with all pairwise comparisons being significant (all p's <.0001). When examining the Stroop Effect (incongruent – congruent trials), there were no significant AD biomarker effects on accuracy or RT that survived the multiple comparisons.

4. Functional Results

4.1 Animacy Task

Block level analyses yielded robust BOLD increases during task performance in visual, motor, and attentional networks, and decreases in the default mode network (DMN) (Figure 2a). When contrasting trial types, animate trials had significantly reduced deactivations of the DMN, whereas inanimate trials had greater increases in motor areas (Figure3a). As word frequency increased there was a smaller deactivation of the precuneus. As frequency decreased there were larger increases in activation the left dorsolateral prefrontal cortex (DLPFC) and visual word form area (Figure 3b). The color scales on the figures were selected to show the dynamic range of the effects and full cluster information for all effects are presented in Supplementary Tables 3-5.

In addition to the frequency and animacy effects, there was a clear subsequent memory effect (see Paller and Wagner, 2002). Specifically, compared to forgotten words, highly confident remembered words evoked greater BOLD signal in the anterior cingulate, medial prefrontal cortex, left entorhinal and parahippocampal cortex, left temporal lobe and extensively in the left DLPFC. Forgotten word trials had smaller deactivations in the precuneus and larger increases in the right angular gyrus (Figure 3c).

4.2 Stroop Task

The block level analyses produced robust activations and deactivations in a near identical network to the Animacy Task (Figure2b). Relative to congruent trials, incongruent trials elicited greater activity in the anterior cingulate, left parietal cortex, left angular gyrus, and bilaterally in the DLPFC (Figure 3d), consistent with meta-analyses of Stroop performance (e.g. Derrfuss et al., 2005)

4.3 Relationship with Biomarkers

Importantly, additional associations with CSF biomarkers and MCBP were examined for the block and trial level fMRI effects. For the block level effects in the Animacy and Stroop tasks there were significant positive associations between levels of tau and ptau in areas activated by the tasks (Figure 4a-4d). These regions were activated relative to baseline, and the level of activation increased with rising levels of tau and ptau. There were no significant block level associations with CSF $A\beta_{42}$ or MCBP. Although the regions that reached statistical significance varied somewhat by task and biomarker (tau vs. ptau), by using a lower statistical threshold it is possible to see that the spatial patterns are remarkably similar across the four maps (see Figure 4 areas in green). It is possibly that the modulation of the block level effects by levels of tau and ptau were driven by a subset of the cohort. In order to address this issue, we used the areas that reached significance in Figure 4a as a region of interest to display the relationship between log ptau and alterations in the BOLD signal across the cohort (Figure 5). This figure indicates a relatively continuous effect of rising levels of pathology on blood flow.

There was only one interaction between trial level effects and biomarkers. When examining the difference between highly confident remembered trials to those later forgotten,

there was a negative association with tau in bilateral motor areas (Figure 4e). This indicated that as tau levels increased the differences between highly confident remembered and forgotten trials became more negative in this region. Cluster information for all effects are presented in Supplementary Tables 3-5.

5. Discussion

The focus of the current research was to examine the presence of functional changes tied to AD pathology using a design that estimated both block and trial level activity. The combination of block and trial level manipulations allowed the examination of large-scale attentional fluctuations, trial level attentional manipulations, as well as estimation of subsequent memory effects. The trial level manipulations produced results consistent with prior work examining animacy (Grossman et al., 2002), word frequency (Kronbichler et al., 2004), subsequent memory (Kim, 2011), and Stroop effects (Derrfuss et al., 2005), but these effects were minimally modulated by levels of AD biomarkers. The block level manipulations produced robust patterns of activation and deactivation correlated with large-scale shifts in sustained attention. Importantly, these block-level effects were related to tau and ptau levels in both tasks. These results occurred in the absence of significant behavioral impairment, as is consistent with prior work examining nondemented individuals with an elevated levels of AD biomarkers or a genetic risk for AD (e.g. Aizenstein et al., 2008; Dennis et al., 2010; Filbey et al., 2010; Han et al., 2007; Mormino et al., 2012; Persson et al., 2008; Reiman et al., 2009).

The tau and ptau modulations were highly co-localized with tissue activated by the task. On average 75% of the voxels that were significantly modulated by tau or ptau were also

activated by their respective task, while less that .05% of the voxels fell in areas that were deactivated. Further it is not just the extent of this overlap that is noteworthy, but the specific regions that produce this overlap. The greatest effects of the AD biomarkers occurred in the right dorsolateral prefrontal cortex, anterior cingulate, and lateral parietal regions, which have long been associated with executive control, attention, and working memory (Banich et al., 2000; Corbetta and Shulman, 2002; Coull and Nobre, 1998; Kane and Engle, 2002; MacDonald et al., 2000; Milham et al., 2002; Pardo et al., 1991; Wager et al., 2004). The modulation of these attentional control networks supports theories that early stages of AD are accompanied by alterations in attentional control (Bäckman et al., 2005; Balota and Faust, 2001; Duchek et al., 2013; Hutchison et al., 2010; Perry and Hodges, 1999).

The present study indicated that across two tasks, individuals with higher levels of AD injury biomarkers over-activated attentional areas. A diffuse or inefficient mobilization of attentional networks would create poorer representations of attended material that in turn would negatively affect memory performance. Due to the high levels of performance, it is unclear whether the observed overactivations represent successful compensatory mechanisms or detrimental effects that have not yet reached a level to impact performance. As with work on aging (Schneider-Garces et al., 2010), future studies using parametric manipulations of difficulty are needed to disentangle such mechanisms.

When examining the difference between remembered and forgotten trials there was a small effect of tau in motor cortex. The relationship was such that the difference between remembered and forgotten trials in this area increased with rising levels of tau. This may reflect a consequence of strategic differences at the time of the initial animacy judgments, which are later predictive of memory. There was also a significant three-way interaction behaviorally with ptau

when examining tests of memory. When faced with unseen words, increasing levels of ptau predicted more rapid incorrect false alarms, but much longer successful correct rejections. This suggests a difficulty overcoming the general sense of familiarity when presented with unseen words.

Prior work in the literature has primarily determined AD risk by the presence of an *APOE* ε4 allele or by high levels of insoluble amyloid measured with PET (Bondi et al., 2005; Bookheimer et al., 2000; Dennis et al., 2010; Filbey et al., 2010; Han et al., 2007; Lind et al., 2006; Mormino et al., 2012; Trivedi et al., 2006). The present study extends such analyses to include CSF markers of AD. Levels of CSF tau and Aβ are minimally correlated, and each has a unique association with amyloid measured with PET (Aschenbrenner et al., 2014; Storandt et al., 2012). Examining both CSF and PET measures provides a more thorough characterization than using only one technique. After controlling for age, gender, and education, levels of tau and ptau correlated with MCBP above .4 (p's<.001). Along with careful subject recruitment and neurological screening, this suggests the elevated tau levels in our sample are representative of AD processes.

This study is the first to relate task-evoked functional changes to levels of tau and ptau. We found that task-evoked alterations in the BOLD signal were most sensitive to tau rather than amyloid pathology in nondemented individuals. This is consistent with prior work indicating that the progression of dementia is not correlated best with amyloid, but rather with synaptic and neuronal loss, which is more tightly coupled with levels of NFTs (Gomez-Isla et al., 1996; Ingelsson et al., 2004; Morris and Price, 2001). Whereas most previous fMRI studies of AD using amyloid PET have focused on explicit memory encoding tasks, here we utilized large-scale manipulations of attention. As tau and amyloid pathology have divergent spatial topographies

(Braak and Braak, 1991) different cognitive domains may be preferentially affected by tau and amyloid pathology. In the future it would be helpful to directly compare memory retrieval to attentional control to assess whether these two cognitive task domains are differentially affected by tau and amyloid pathology.

Increased levels of tau and ptau were linked to widespread block level modulations of the BOLD signal, but had minimal interactions with trial level effects. There are two potential interpretations of this pattern. The first is that pathological processes affect gross attentional modulation while sparing focal trial-to-trial allocations of resources. A second interpretation is that detrimental processes are occurring at both levels, but the current design is more sensitive to large-scale shifts compared to subtle differences across trial types.

There are some limitations to the present study. First, this study examined a cross-sectional relationship between measures of AD pathology and altered fMRI activity. It may be that the longitudinal trajectories of the pathological markers are more related to alteration in attentional control. Additionally, although the lag between PET and MRI sessions was minimal, a subset of individuals had relatively long lags between CSF collection and the MRI. To address this variability, all statistical models examining biomarkers included the lag between an individual's MRI and biomarker session as a covariate. As an additional test, we split the data presented in Figure 5 into two groups: individuals with a CSF-to-MRI lag less than or greater than two years. In this model, again including age, gender, and education as covariates, the relationship between levels of ptau and BOLD modulation remain highly significant ($F_{1,59}$ 48.49, $p < .00001$) and there was no modulation of this relationship by lag group ($F_{1,59} = 1.02$, $p = .32$) (See Figure 6). This indicates that at least within the current lag ranges, there is no systematic change in the CSF biomarker-block level fMRI relationship.

In the present study we have focused on attentional control systems due to accumulating evidence that attention plays a critical role in early stage AD (see Balota and Ducheck, 2014). Indeed, during the current Animacy and Stroop tasks we observed alterations in task-evoked activity related to AD biomarkers even though there was relatively little demand on memory systems. Since there is a critical link between attention and memory processing (Craik and Lockhart, 1972; Jacoby, 1991), these alterations in block-level sustained attention may ultimately be a predictor of later disruptions of memory processing. Following our cohort longitudinally will provide insight into the utility of using overactivations of attentional control networks to predict subsequent cognitive decline. Finally, studies in the field should consider combining encoding tasks with very little memory demand with memory retrieval tasks to examine the sensitivity of attention and/or memory to AD pathology.

Great strides have been made characterizing early AD abnormalities *in vivo* using structural and functional magnetic resonance imaging, PET, CSF assays, and cognitive tests (Holtzman et al., 2011). Efforts are underway to integrate these techniques to develop biomarkers to aid in disease diagnosis, prognosis, and prevention. As CSF assays and PET tau tracers become more widespread, it will be possible to determine if neural measures of tau and amyloid pathology preferentially affect different functional and cognitive systems. Exploring sustained attention may be sensitive to these very early biomarkers of AD.

6. Acknowledgements

The authors thank Allison Midden, Andy Aschenbrenner, Patricia Stevenson, and Kelley Jackonson for helping run study participants and providing general assistance to the project including regulatory management, and the Biomarker, Clinical, Genetics and Imaging Cores

7. Study Funding

Research reported in this publication was supported by NIH grant P01 AG026276, NIA T32AG00035, and Washington University Institute of Clinical and Translational Sciences grant UL1 TR000448 from the National Center for Advancing Translational Sciences (NCATS). This work used the services of the Neuroimaging Informatics and Analysis Center, supported by NIH grant 5P30NS048056. Generous support was provided by Fred Simmons and Olga Mohan and by Charles F. and Joanne Knight Alzheimer's Research Initiative. The content is solely the responsibility of the authors and does not necessarily represent the official view of the NIH.

Table 1. Demographics of the study cohort.

N=71 Female = 44 (62%) APOE ε4+= 22 (31%)				
	Mean	Median	Range	Abnormal (%)
Age (years)	63.5	63	49-78	
Education (years)	15.5	16	12-20	
MMSE	29.5	30	26-30	
$A\beta_{42}$ (pg/ml)	770.4	779.0	285.3-1360.5	15.5%
Tau (pg/ml)	250.4	225.7	100.0-588.3	21.1%
$Ptau_{181}$ (pg/ml)	53.5	48.5	24.8-127.2	16.9%
CSF Lag (days)	474	161	1-2227	
MCBP	.29	.13	.02-1.32	25.4%
PET Lag (days)	39	0	0-415	

MCBP = PiB mean cortical binding potential
Lag = days between MRI and biomarker assessment
MMSE = mini-mental states exam

Table 2. Mean accuracy (ACC), reaction time (RT) and standardized RT (zRT) as a function of condition in the Animacy Judgment task and in the Stroop Task. Values represent marginal means and standard errors (in parentheses).

Animacy Task

	High Animate	Low Animate	High Inanimate	Low Inanimate
ACC	.96 (.01)	.93 (.01)	.97 (.01)	.96 (.01)
RT (msec)	888 (13.52)	970 (15.04)	983 (14.5)	1047 (16.18)
zRT	-.43 (.02)	-.04 (.02)	.05 (.02)	.35 (.02)

Memory Test

	Old Accurate	Old Inaccurate	New Accurate	New Inaccurate
Proportion	.76 (.02)	.24 (.02)	.74 (.02)	.26 (.02)
RT (msec)	2123 (65.48)	2869 (100.20)	2611 (84.33)	2778 (103.13)
zRT	-.21 (.02)	.37 (.04)	.14 (.03)	.26 (.04)
Confidence	4.33 (.07)	3.31 (.10)	3.59 (.11)	3.65 (.09)

Stroop Task

	Congruent	Neutral	Incongruent	Stroop Effect
ACC	.99 (.00)	.99 (.00)	.97 (.00)	.02 (.00)
RT (msec)	743. (12.76)	759 (13.29)	845 (15.88)	102 (6.0)
zRT	-.23 (.02)	-.13 (.02)	.36 (.02)	.58 (.03)

Table 3. Results from statistical models examining the relationship between performance in the Animacy Judgment task, Subsequent Memory Recognition task, and the Stroop task for each of the biomarkers. P-values are uncorrected for multiple comparisons.

Animacy

		$A\beta_{42}$	Tau	$Ptau_{181}$	MCBP
Main Effect	*ACC*	$F_{1,60}$=.00,	$F_{1,60}$=.37	$F_{1,60}$=2.27	$F_{1,60}$=1.96
	zRT	$F_{1,60}$=.11	$F_{1,60}$=.07	$F_{1,60}$=.28	$F_{1,60}$=.58
Biomarker x Animacy	*ACC*	$F_{1,60}$=.10	$F_{1,60}$=.03	$F_{1,60}$=.50	$F_{1,60}$=3.19
	zRT	$F_{1,60}$=.05	$F_{1,60}$=.01	$F_{1,60}$=.09	$F_{1,60}$=.05
Biomarker x Frequency	*ACC*	$F_{1,60}$=.04	$F_{1,60}$=1.58	$F_{1,60}$=1.25	$F_{1,60}$=.46
	zRT	$F_{1,60}$=.62	$F_{1,60}$=.05	$F_{1,60}$=.01	$F_{1,60}$=1.79
3-Way Interaction	*ACC*	$F_{1,60}$=.28	$F_{1,60}$=1.71	$F_{1,60}$=.93	$F_{1,60}$=.11
	zRT	$F_{1,60}$=.05	$F_{1,60}$=.00	$F_{1,60}$=.29	$F_{1,60}$=.62

Memory

		$A\beta_{42}$	Tau	$Ptau_{181}$	MCBP
Main Effect	ACC	$F_{1,60}$=3.23	$F_{1,60}$=.21	$F_{1,60}$=.14	$F_{1,60}$=.22
	zRT	$F_{1,60}$=.40	$F_{1,60}$=.18	$F_{1,60}$=.11	$F_{1,60}$=.37
	Confidence	$F_{1,60}$=.34	$F_{1,60}$=.87	$F_{1,60}$=.00	$F_{1,60}$=.58
Biomarker x by Old/New	ACC	$F_{1,60}$=.08	$F_{1,60}$=.61	$F_{1,60}$=.23	$F_{1,60}$=.86
	zRT	$F_{1,60}$=.30	$F_{1,60}$=7.03*****	$F_{1,60}$=7.18*****	$F_{1,60}$=.39
	Confidence	$F_{1,60}$=1.09	$F_{1,60}$=1.87	$F_{1,60}$=1.40	$F_{1,60}$=.02
Biomarker x Accuracy	zRT	$F_{1,60}$=1.12	$F_{1,60}$=1.68	$F_{1,60}$=.01	$F_{1,60}$=.13
	Confidence	$F_{1,60}$=.01	$F_{1,60}$=.20	$F_{1,60}$=.00	$F_{1,60}$=.21
Biomarker x Accuracy x Old/New	zRT	$F_{1,60}$=.00	$F_{1,60}$=6.58 *****	$F_{1,60}$=6.75 *****	$F_{1,60}$=2.58
	Confidence	$F_{1,60}$=.13	$F_{1,60}$=.85	$F_{1,60}$=.74	$F_{1,60}$=.36

Stroop

		$A\beta_{42}$	Tau	$Ptau_{181}$	MCBP
Main Effect	*ACC*	$F_{1,58}$=.86	$F_{1,58}$=1.31	$F_{1,58}$=.42	$F_{1,58}$=.45
	zRT	$F_{1,58}$=.01	$F_{1,58}$=.69	$F_{1,58}$=.32	$F_{1,58}$=.15
Stoop Effect	*ACC*	$F_{1,58}$=1.43	$F_{1,58}$=.19	$F_{1,58}$=.27	$F_{1,58}$=3.81
	zTotal	$F_{1,58}$=4.53^{+}	$F_{1,58}$=.10	$F_{1,58}$=1.79	$F_{1,58}$=3.29

zRT = z-transformed reaction time data
ACC = Fisher's transformed accuracy data MCBP = mean cortical PIB binding potential
$^{+}$ = p <.05, * p<.01

Figure Legends

Figure 1. Schematic depicting overview of experimental sessions.

Figure 2. Block Level fMRI Effects. Warm colors represent areas more active during task intervals while those in cool colors are more active during rest intervals for the A) Animacy and B) Stroop tasks.

Figure 3. Trial Level fMRI Effects. A) Areas in warm colors were more active for animate trials while those in blue were more active for inanimate trials. B) Areas positively and negatively associated with word frequency. C) Areas in warm colors were more active for later remembered trials with high confidence, while those in cool colors were more active for later forgotten trials. D) Areas demonstrating increased activity to incongruent relative to congruent Stroop trials.

Figure 4. Alzheimer Biomarker Effects. In the Animacy task, areas positively associated with CSF A) ptau and B) tau. In the Stroop task, areas positively associated with CSF C) ptau and D) tau. E) A modulation by tau of the difference between highly confident remembered and forgotten trials. For all figures, areas in green indicate additional statistical effects using a more lenient threshold of z=1.8.

Figure 5. Ptau modulations of the BOLD signal across the cohort in the Animacy Task. Values on the x-axis represent log ptau residuals after controlling for age, gender, and education. The y-axis depicts the BOLD modulation residuals after controlling for the same variables.

Figure 6. Ptau modulations of the BOLD signal separated by time lag. Values on the x-axis represent log ptau residuals after controlling for age, gender, and education. The y-axis

depicts the BOLD modulation residuals after controlling for the same variables. Circles and a solid line represent individuals with a lag between CSF collection and MRI less than two years. Diamonds and the dashed line slow represent individuals with a lag greater than two years.

Citations

Aizenstein, H.J., Nebes, R.D., Saxton, J. a, Price, J.C., Mathis, C. a, Tsopelas, N.D., Ziolko, S.K., James, J. a, Snitz, B.E., Houck, P.R., Bi, W., Cohen, A.D., Lopresti, B.J., DeKosky, S.T., Halligan, E.M., Klunk, W.E., 2008. Frequent amyloid deposition without significant cognitive impairment among the elderly. Arch. Neurol. 65, 1509–17.

Albert, M.S., Moss, M.B., Tanzi, R.E., Jones, K., 2001. Preclinical prediction of AD using neuropsychological tests. J. Int. Neuropsychol. Soc. 7, 631–639.

Aschenbrenner, A.J., Balota, D.A., Tse, C.-S., Fagan, A.M., Holtzman, D.M., Benzinger, T.L.S., Morris, J.C., 2014. Alzheimer disease biomarkers, attentional control, and semantic memory retrieval: synergistic and mediational effects of biomarkers on a sensitive cognitive measure in non-demented older adults. Neuropsychology.

Bäckman, L., Jones, S., Berger, A.-K., Laukka, E.J., Small, B.J., 2005. Cognitive impairment in preclinical Alzheimer's disease: a meta-analysis. Neuropsychology 19, 520–31.

Balota, D.A., Ducheck, J.M., 2014. Attention variability, and biomarkers in Alzheimer's disease, in: Lindsay, D., Kelley, C., Yonelinas, A.P., Roediger, Henry L., I. (Eds.), Remembering: Attributions, Processes, and Control in Human Memory. Psychology Press, New York, NY.

Balota, D.A., Faust, M.E., 2001. Attention in dementia of the Alzheimer's type, in: Boller, F., Cappa, S. (Eds.), Handbook of Neuropsychology. Elsevier Science, New York, NY, pp. 51–80.

Balota, D.A., Tse, C.-S., Hutchison, K.A., Spieler, D.H., Duchek, J.M., Morris, J.C., 2010. Predicting conversion to dementia of the Alzheimer's type in a healthy control sample: the power of errors in Stroop color naming. Psychol. Aging 25, 208–18.

Banich, M.T., Milham, M.P., Atchley, R., Cohen, N.J., Webb, A., Wszalek, T., Kramer, A.F., Liang, Z.-P., Wright, A., Shenker, J., Magin, R., 2000. fMRI studies of stroop tasks reveal unique roles of anterior and posterior brain systems in attentional selection. J. Cogn. Neurosci. 12, 988–1000.

Bateman, R.J., Xiong, C., Benzinger, T.L.S., Fagan, A.M., Goate, A., Fox, N.C., Marcus, D.S., Cairns, N.J., Xie, X., Blazey, T.M., Holtzman, D.M., Santacruz, A., Buckles, V., Oliver, A., Moulder, K., Aisen, P.S., Ghetti, B., Klunk, W.E., McDade, E., Martins, R.N., Masters, C.L., Mayeux, R., Ringman, J.M., Rossor, M.N., Schofield, P.R., Sperling, R. a, Salloway, S., Morris, J.C., 2012. Clinical and biomarker changes in dominantly inherited Alzheimer's disease. N. Engl. J. Med. 367, 795–804.

Benzinger, T.L.S., Blazey, T., Jack, C.R., Koeppe, R.A., Su, Y., Xiong, C., Raichle, M.E., Snyder, A.Z., Ances, B.M., Bateman, R.J., Cairns, N.J., Fagan, A.M., Goate, A., Marcus, D.S., Aisen, P.S., Christensen, J.J., Ercole, L., Hornbeck, R.C., Farrar, A.M., Aldea, P., Jasielec, M.S., Owen, C.J., Xie, X., Mayeux, R., Brickman, A., McDade, E., Klunk, W.,

Mathis, C. a, Ringman, J., Thompson, P.M., Ghetti, B., Saykin, A.J., Sperling, R.A., Johnson, K.A., Salloway, S., Correia, S., Schofield, P.R., Masters, C.L., Rowe, C., Villemagne, V.L., Martins, R., Ourselin, S., Rossor, M.N., Fox, N.C., Cash, D.M., Weiner, M.W., Holtzman, D.M., Buckles, V.D., Moulder, K., Morris, J.C., 2013. Regional variability of imaging biomarkers in autosomal dominant Alzheimer's disease. Proc. Natl. Acad. Sci. U. S. A. 110, E4502–4509.

Birks, J., 2006. Cholinesterase inhibitors for Alzheimer's disease. Cochrane database Syst. Rev. CD005593.

Bondi, M.W., Houston, W.S., Eyler, L.T., Brown, G.G., 2005. fMRI evidence of compensatory mechanisms in older adults at genetic risk for Alzheimer disease. Neurology 64, 501–8.

Bookheimer, S.Y., Strojwas, M.H., Cohen, M.S., Sanders, A., Pericak-Vance, M.A., Mazziotta, J.C., Small, G.W., Saunders, A.M., 2000. Patterns of Brain Activations in People at Risk for Alzheimer's Disease. N. Engl. J. Med. 343, 450–456.

Braak, H., Braak, E., 1991. Neuropathological stageing of Alzheimer-related changes. Acta Neuropathol. 239–259.

Corbetta, M., Shulman, G.L., 2002. Control of goal-directed and stimulus-driven attention in the brain. Nat. Rev. Neurosci. 3, 201–15.

Coull, J.T., Nobre, A.C., 1998. Where and when to pay attention: the neural systems for directing attention to spatial locations and to time intervals as revealed by both PET and fMRI. J. Neurosci. 18, 7426–35.

Craik, F.I.M., Lockhart, R.S., 1972. Levels of processing: A framework for memory research. J. Verbal Learning Verbal Behav. 11, 671–684.

Dennis, N.A., Browndyke, J.N., Stokes, J., Need, A., Burke, J.R., Welsh-Bohmer, K. a, Cabeza, R., 2010. Temporal lobe functional activity and connectivity in young adult APOE varepsilon4 carriers. Alzheimer's Dement. 6, 303–11.

Derrfuss, J., Brass, M., Neumann, J., von Cramon, D.Y., 2005. Involvement of the inferior frontal junction in cognitive control: meta-analyses of switching and Stroop studies. Hum. Brain Mapp. 25, 22–34.

Duchek, J.M., Balota, D. a, Thomas, J.B., Snyder, A.Z., Rich, P., Benzinger, T.L., Fagan, A.M., Holtzman, D.M., Morris, J.C., Ances, B.M., 2013. Relationship between Stroop performance and resting state functional connectivity in cognitively normal older adults. Neuropsychology 27, 516–28.

Fagan, A.M., Mintun, M.A., Mach, R.H., Lee, S.-Y., Dence, C.S., Shah, A.R., LaRossa, G.N., Spinner, M.L., Klunk, W.E., Mathis, C.A., DeKosky, S.T., Morris, J.C., Holtzman, D.M.,

2006. Inverse relation between in vivo amyloid imaging load and cerebrospinal fluid Aβ42 in humans. Ann. Neurol. 59, 512–519.

Faust, M.E., Ferraro, F.R., Balota, D.A., Spieler, D.H., 1999. Individual differences in information-processing rate and amount: Implications for group differences in response latency. Psychol. Bull. 125, 777–799.

Filbey, F.M., Chen, G., Sunderland, T., Cohen, R.M., 2010. Failing compensatory mechanisms during working memory in older apolipoprotein E-epsilon4 healthy adults. Brain Imaging Behav. 4, 177–88.

Fischl, B., 2004. Automatically Parcellating the Human Cerebral Cortex. Cereb. Cortex 14, 11–22.

Gomez-Isla, T., Price, J.L., Mckeel, D.W., Morris, J.C., Growdon, J.H., Hyman, B.T., 1996. Profound loss of layer II entorhinal cortex neurons occurs in very mild Alzheimer's disease. J. Neurosci. 16, 4491–4500.

Grossman, M., Koenig, P., DeVita, C., Glosser, G., Alsop, D., Detre, J., Gee, J., 2002. The neural basis for category-specific knowledge: an fMRI study. Neuroimage 15, 936–48.

Han, S.D., Houston, W.S., Jak, A.J., Eyler, L.T., Nagel, B.J., Fleisher, A.S., Brown, G.G., Corey-Bloom, J., Salmon, D.P., Thal, L.J., Bondi, M.W., 2007. Verbal paired-associate learning by APOE genotype in non-demented older adults: fMRI evidence of a right hemispheric compensatory response. Neurobiol. Aging 28, 238–47.

Hardy, J.A., Higgins, G.A., 1992. Alzheimer's disease: The amyloid cascade hypothesis. Science (80-.).

Himmelheber, A.M., Sarter, M., Bruno, J.P., 2000. Increases in cortical acetylcholine release during sustained attention performance in rats. Cogn. Brain Res. 9, 313–325.

Holtzman, D., Morris, J.C., Goate, A.M., 2011. Alzheimer's Disease : The Challenge of the Second Century. Sci. Transl. Med. 3, 1–17.

Hutchison, K.A., Balota, D.A., Duchek, J.M., Ducheck, J.M., 2010. The utility of Stroop task switching as a marker for early-stage Alzheimer's disease. Psychol. Aging 25, 545–59.

Ingelsson, M., Fukumoto, H., Newell, K.L., Growdon, J.H., Hedley-Whyte, E.T., Frosch, M.P., Albert, M.S., Hyman, B.T., Irizarry, M.C., 2004. Early Aβ accumulation and progressive synaptic loss, gliosis, and tangle formation in AD brain. Neurology 62, 925–931.

Jack, C.R., Knopman, D.S., Jagust, W.J., Petersen, R.C., Weiner, M.W., Aisen, P.S., Shaw, L.M., Vemuri, P., Wiste, H.J., Weigand, S.D., Lesnick, T.G., Pankratz, V.S., Donohue, M.C., Trojanowski, J.Q., 2013. Tracking pathophysiological processes in Alzheimer's disease: an updated hypothetical model of dynamic biomarkers. Lancet Neurol. 12, 207–16.

Jacoby, L.L., 1991. A process dissociation framework: Separating automatic from intentional uses of memory. J. Mem. Lang. 30, 513–541.

Jenkinson, M., Beckmann, C.F., Behrens, T.E.J., Woolrich, M.W., Smith, S.M., 2012. FSL. Neuroimage 62, 782–90.

Kaduszkiewicz, H., Zimmermann, T., Beck-Bornholdt, H.-P., van den Bussche, H., 2005. Cholinesterase inhibitors for patients with Alzheimer's disease: systematic review of randomised clinical trials. BMJ 331, 321–7.

Kane, M.J., Engle, R.W., 2002. The role of prefrontal cortex in working-memory capacity, executive attention, and general fluid intelligence: An individual-differences perspective. Psychon. Bull. Rev. 9, 637–671.

Kim, H., 2011. Neural activity that predicts subsequent memory and forgetting: a meta-analysis of 74 fMRI studies. Neuroimage 54, 2446–61.

Kronbichler, M., Hutzler, F., Wimmer, H., Mair, A., Staffen, W., Ladurner, G., 2004. The visual word form area and the frequency with which words are encountered: evidence from a parametric fMRI study. Neuroimage 21, 946–53.

Lind, J., Persson, J., Ingvar, M., Larsson, A., Cruts, M., Van Broeckhoven, C., Adolfsson, R., Bäckman, L., Nilsson, L.-G., Petersson, K.M., Nyberg, L., 2006. Reduced functional brain activity response in cognitively intact apolipoprotein E epsilon4 carriers. Brain 129, 1240–8.

MacDonald, A.W., Cohen, J.D., Stenger, A., Carter, C.S., 2000. Dissociating the role of the dorsolateral prefrontal and anterior cingulate cortex in cognitive control. Science (80-.). 288, 1835–1838.

Milham, M.P., Erickson, K.I., Banich, M.T., Kramer, A.F., Webb, A., Wszalek, T., Cohen, N.J., 2002. Attentional control in the aging brain: insights from an fMRI study of the Stroop task. Brain Cogn. 49, 277–296.

Mormino, E.C., Brandel, M.G., Madison, C.M., Marks, S., Baker, S.L., Jagust, W.J., 2012. Aβ Deposition in aging is associated with increases in brain activation during successful memory encoding. Cereb. Cortex 22, 1813–23.

Morris, J., Price, J.L., 2001. Pathologic correlates of nondemented aging , mild cognitive impairment , and early-stage Alzheimer's Disease. J. Mol. Neurosci. 17, 101–118.

Morris, J.C., 1993. The Clinical Dementia Rating (CDR): Current version and scoring rules. Neurology 43, 2412–2414.

Paller, K.A., Wagner, A.D., 2002. Observing the transformation of experience into memory. Trends Cogn. Sci. 6, 93–102.

Pardo, J. V, Fox, P.T., Raichle, M.E., 1991. Localization of a human system for sustained attention by positron emission tomography. Nature 349, 61–4.

Perry, R.J., Hodges, J.R., 1999. Attention and executive deficits in Alzheimer's disease A critical review. Brain 122, 383–404.

Persson, J., Lind, J., Larsson, A., Ingvar, M., Sleegers, K., Van Broeckhoven, C., Adolfsson, R., Nilsson, L.-G., Nyberg, L., 2008. Altered deactivation in individuals with genetic risk for Alzheimer's disease. Neuropsychologia 46, 1679–1687.

Reiman, E.M., Chen, K., Liu, X., Bandy, D., Yu, M., Lee, W., Ayutyanont, N., Keppler, J., Reeder, S.A., Langbaum, J.B.S., Alexander, G.E., Klunk, W.E., Mathis, C.A., Price, J.C., Aizenstein, H.J., DeKosky, S.T., Caselli, R.J., 2009. Fibrillar amyloid-beta burden in cognitively normal people at 3 levels of genetic risk for Alzheimer's disease. Proc. Natl. Acad. Sci. U. S. A. 106, 6820–5.

Sahakian, B., Jones, G., Levy, R., Gray, J., Warburton, D., 1989. The effects of nicotine on attention, information processing, and short-term memory in patients with dementia of the Alzheimer type. Br. J. Psychiatry 154, 797–800.

Sarazin, M., Berr, C., De Rotrou, J., Fabrigoule, C., Pasquier, F., Legrain, S., Michel, B., Puel, M., Volteau, M., Touchon, J., Verny, M., Dubois, B., 2007. Amnestic syndrome of the medial temporal type identifies prodromal AD: a longitudinal study. Neurology 69, 1859–67.

Sarter, M., Bruno, J.P., 1997. Cognitive functions of cortical acetylcholine: toward a unifying hypothesis. Brain Res. Rev. 23, 28–46.

Schneider-Garces, N.J., Gordon, B. a, Brumback-Peltz, C.R., Shin, E., Lee, Y., Sutton, B.P., Maclin, E.L., Gratton, G., Fabiani, M., 2010. Span, CRUNCH, and beyond: working memory capacity and the aging brain. J. Cogn. Neurosci. 22, 655–69.

Selden, N.R., Gitelman, D.R., Salamon-Murayama, N., Parrish, T.B., Mesulam, M.M., 1998. Trajectories of cholinergic pathways within the cerebral hemispheres of the human brain. Brain 121 (Pt 1, 2249–57.

Storandt, M., Head, D., Fagan, A.M., Holtzman, D.M., Morris, J.C., 2012. Toward a multifactorial model of Alzheimer disease. Neurobiol. Aging 33, 2262–71.

Stroop, J.R., 1935. Studies of interference in serial verbal reactions. J. Exp. Psychol. 18, 643–662.

Su, Y., D'Angelo, G.M., Vlassenko, A.G., Zhou, G., Snyder, A.Z., Marcus, D.S., Blazey, T.M., Christensen, J.J., Vora, S., Morris, J.C., Mintun, M. a, Benzinger, T.L.S., 2013. Quantitative Analysis of PiB-PET with FreeSurfer ROIs. PLoS One 8, e73377.

Trivedi, M.A., Schmitz, T.W., Ries, M.L., Torgerson, B.M., Sager, M.A., Hermann, B.P., Asthana, S., Johnson, S.C., 2006. Reduced hippocampal activation during episodic encoding in middle-aged individuals at genetic risk of Alzheimer's disease: a cross-sectional study. BMC Med. 4, 1.

Vos, S.J., Xiong, C., Visser, P.J., Jasielec, M.S., Hassenstab, J., Grant, E.A., Cairns, N.J., Morris, J.C., Holtzman, D.M., Fagan, A.M., 2013. Preclinical Alzheimer's disease and its outcome: a longitudinal cohort study. Lancet Neurol. 12, 957–65.

Wager, T.D., Jonides, J., Reading, S., 2004. Neuroimaging studies of shifting attention: a meta-analysis. Neuroimage 22, 1679–93.

Woolrich, M.W., Behrens, T.E.J., Beckmann, C.F., Jenkinson, M., Smith, S.M., 2004. Multilevel linear modelling for FMRI group analysis using Bayesian inference. Neuroimage 21, 1732–47.

Worsley, K.J., Evans, A.C., Marrett, S., Neelin, P., 1992. A three-dimensional statistical analysis for CBF activation studies in human brain. J. Cereb. Blood Flow Metab. 12, 900–918.

Figure 1

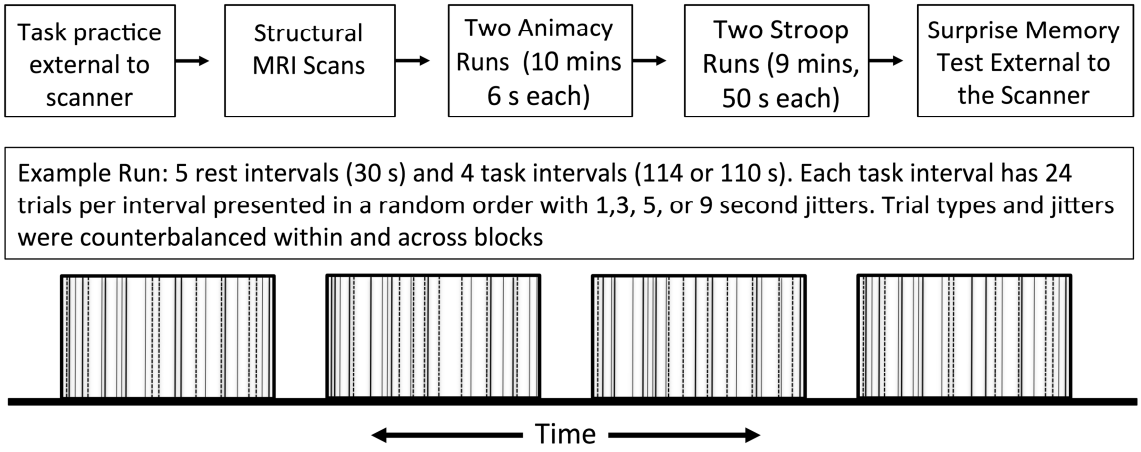

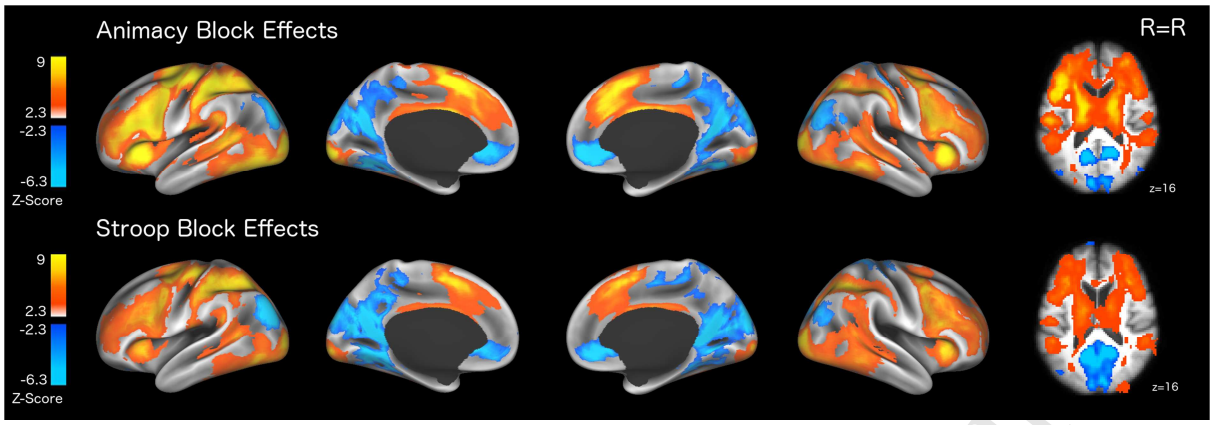

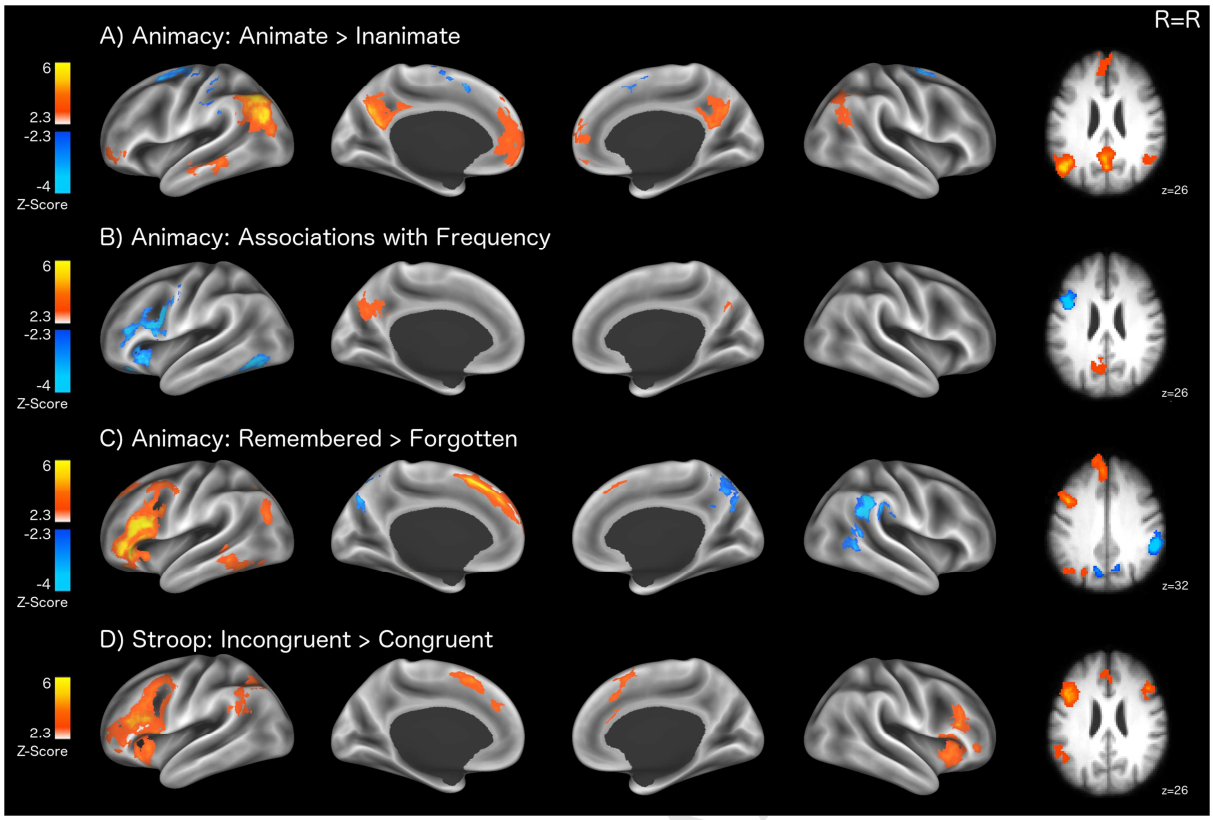

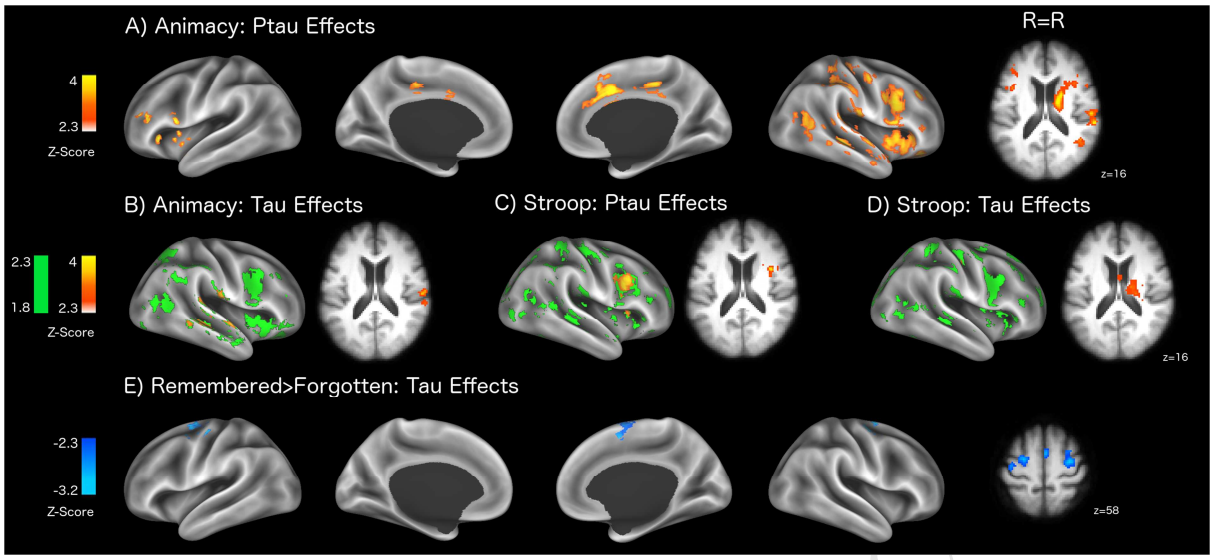

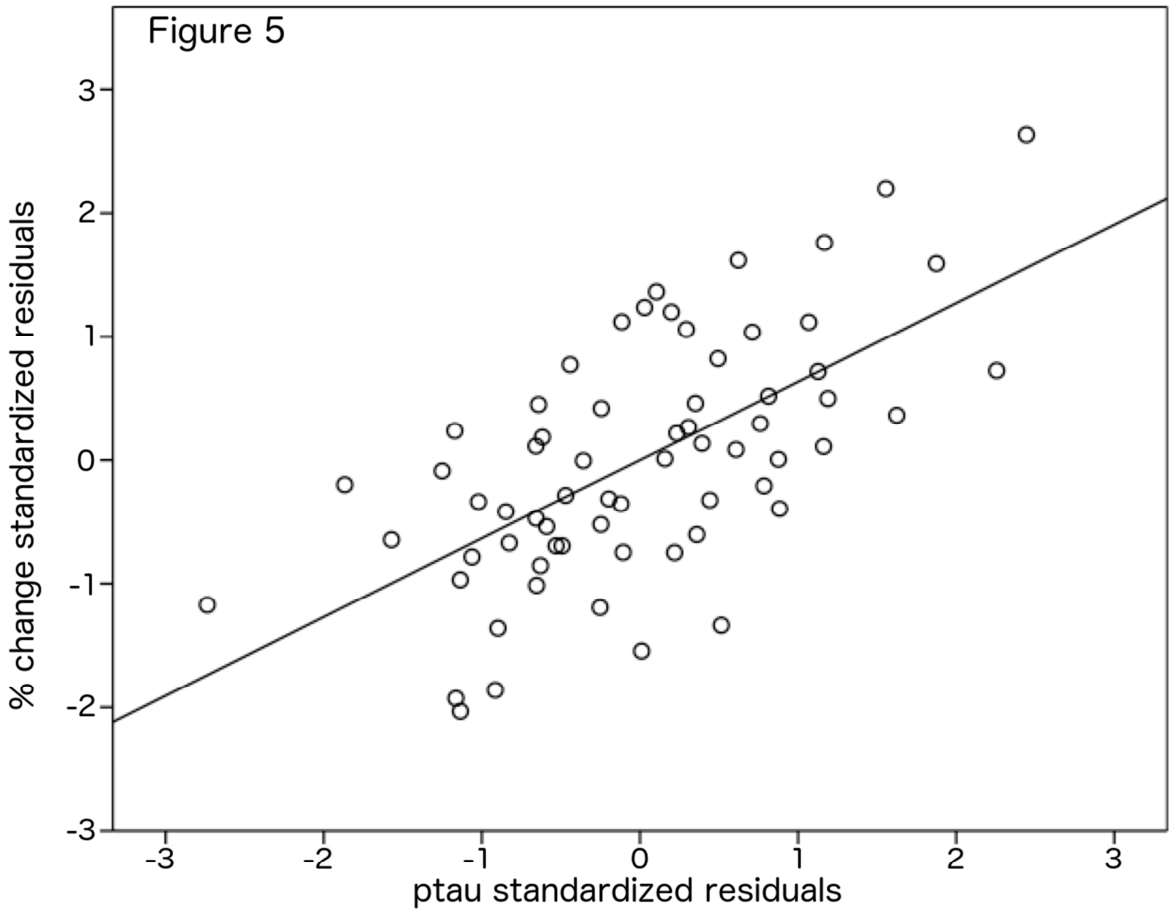
Figure 5
% change standardized residuals
ptau standardized residuals
3
2
1
0
-1
-2
-3
-3
-2
-1
0
1
2
3

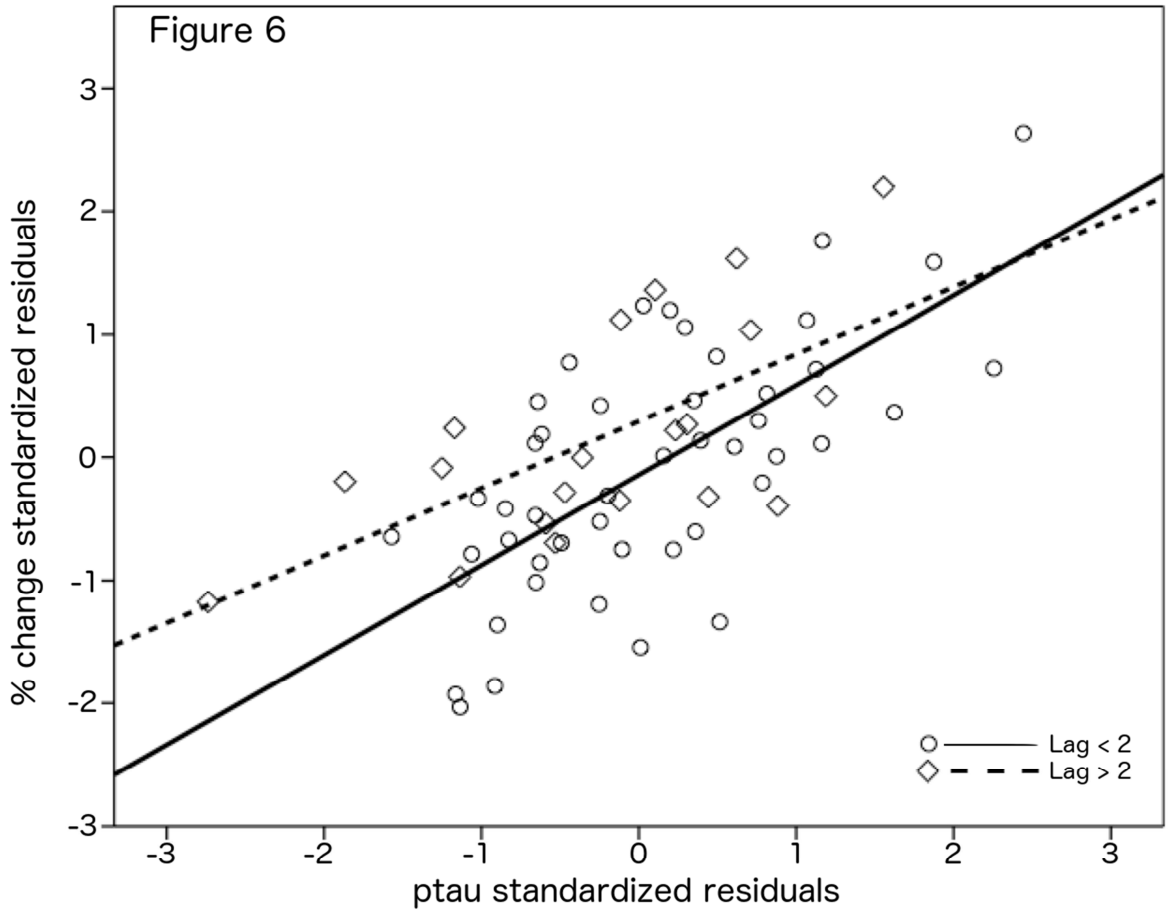
Figure 6
% change standardized residuals
ptau standardized residuals
3
2
1
0
-1
-2
-3
-3
-2
-1
0
1
2
3
Lag < 2
Lag > 2

Supplementary Tables

Supplementary Table 1: Summary memory effects broken down by animacy and frequency.

		High Animate	Low Animate	High Inanimate	Low Inanimate	Inaccurate
ACC	Old	.79 (.02)	.85 (.01)	.66 (.02)	.73 .02)	.24 (.02)
	New	.62 (.02)	.68 (.02)	.80 (.02)	.83 (.02)	.26 (.02)
RT (ms)	Old	1985.9 (66.9)	1906.3 (56.6)	2237.2 (66.0)	2198.0 (75.3)	2842.6 (96.4)
	New	2729.4 (97.5)	2680.6 (93.7)	2520.0 (81.4)	2389.1 (67.9)	2738.6 (99.2)
zRT	Old	-.31 (.03)	-.35 (.02)	-.09 (.03)	-.13 (.03)	.37 (.04)
	New	.26 (.03)	.20 (.03)	.08 (.03)	.03 (.03)	.27 (.04)
Confidence	Old	4.4 (.07)	4.47 (.07)	4.22 (.08)	4.38 (.07)	3.32 (.10)
	New	3.5 (.10)	3.59 (.10)	3.56 (.10)	3.76 (.10)	3.67 (.09)

zRT = z-transformed reaction time data ACC = Fisher's transformed accuracy data

Supplementary Table 2. Effects of animacy and frequency on memory performance

		ACC	zRT	Confidence
Main Effects				
	Animacy	$F_{1,62\ 1,62}$ =1.12	$F_{1,62}$ =.96	$F_{1,62}$ =.67
	Frequency	$F_{1,62}$ =21.22*	$F_{1,62}$ =13.7*	$F_{1,62}$ =79.10*
	Old New	$F_{1,62}$ =.04	$F_{1,62}$ =80.1*	$F_{1,62}$ =104.93*
2-Way				
	Animacy x Frequency	$F_{1,62}$ =.73	$F_{1,62}$ =.00	$F_{1,62}$ =13.35*
	Animacy x Old New	$F_{1,62}$ =176.73*	$F_{1,62}$ =136.39*	$F_{1,62}$ =64.83*
	Frequency x Old new	$F_{1,62}$ =.19	$F_{1,62}$ =.40	$F_{1,62}$ =.97
3-way				
	Animacy x Frequency x Old New	$F_{1,62}$ =.70	$F_{1,62}$ =.06	$F_{1,62}$ =.66

zRT = z-transformed reaction time data ACC = Fisher's transformed accuracy data
* p <.001

Supplementary Table 3: Coordinates for maximal Animacy and Stroop Block data. Coordinates reflect ten maximal foci with data thresholded with a z=8 for task positive regions and z=-5 for task negative regions. Cortical labels come from the Harvard-Oxford atlas.

# Voxels	Log(p)	Max z	x	y	z	Region	Hemisphere
Animacy Block Data							
Positive							
-	42.8	9.96	-38	-20	58	precentral gyrus	L
-	24	10.2	0	10	54	paracentral gyrus	L
-	22.3	9.92	24	-52	-22	insular cortex	L
-	19.2	10.3	-36	20	2	cerebellum	R
-	17.6	9.34	-22	-90	2	insular cortex	R
-	16.6	9.73	32	24	6	inferior frontal gyrus	L
-	12.8	8.88	-16	-10	18	occipital pole	L
-	12.4	8.61	-42	-66	-10	precentral gyrus	L
-	12.2	8.71	26	-90	6	inferior frontal gyrus	L
-	11.6	8.58	18	-64	-46	postcentral gyrus	L
Negative							
-	26.6	-7.38	12	-62	24	precuneus	R
-	22.6	-7.94	0	32	-6	anterior cingulate gyrus	L (midline)
-	15	-7.12	10	-88	24	occipital pole	R
-	11.4	-6.92	-22	-58	-6	lingual gyrus	L
-	11.1	-6.31	-36	-76	32	lateral occipital cortex	L
-	10.6	-6.72	-6	-90	24	occipital pole	L
-	8.26	-6.62	24	-44	-8	lingual gyrus	R
-	3.36	-5.46	6	-36	52	lateral occipital cortex	R
-	2.03	-5.19	40	-76	28	precuneus	R (midline)
-	1.87	-5.02	2	-58	50	lateral occipital cortex	R
Stroop Block Data							
Positive							
-	14.2	8.57	-40	-44	48	superior parietal lobule	L
-	13	8.83	-38	-24	50	postcentral gyrus	L
-	12.2	8.76	18	-52	-18	cerebellum	R
-	11.7	8.53	-28	-58	48	superior parietal lobule	L
-	11.5	8.68	30	-86	6	lateral occipital cortex	R
-	11.5	8.6	-26	-88	0	lateral occipital cortex	L
-	11.1	8.47	-4	6	52	supplementary motor cortex	L (midline)
-	10.2	8.23	34	-48	42	superior parietal lobule	R
-	10.2	8.25	34	24	8	frontal operculum cortex	R
-	10.1	8.27	-44	-24	46	postcentral gyrus	L
Negative							
-	51.3	-7.99	12	-56	16	precuneous	R (midline)
-	15.6	-7.41	-36	-76	34	lateral occipital cortex	L
-	13.3	-6.12	8	40	-2	anterior cingulate gyrus	R (midline)
-	8.98	-5.23	-8	-92	24	occipital pole	L (midline)
-	2.84	-4.59	18	-66	-2	lingual gyrus	R
-	2.22	-5.22	-12	-38	48	postcentral gyrus	L
-	2.22	-4.81	40	-74	28	lateral occipital cortex	R
-	2.08	-4.51	30	-32	-14	parahippocampal gyrus	R
-	1.92	-4.79	-14	-78	40	lateral occipital cortex	L
-	1.92	-4.41	-14	-90	34	occipital pole	L

Supplementary Table 4: Coordinates for all trial level data. Cortical labels come from the Harvard-Oxford atlas.

# Voxels	-log(p)	Max Z	x	y	z	LABEL	Hemisphere
Animate							
2946	9.51	4.16	0	56	-8	frontal pole	L (midline)
2743	8.97	5.75	-48	-66	28	lateral occipital cortex	L
1950	6.75	5.31	0	-66	30	precuneus	L (midline)
955	3.46	3.75	34	-60	48	lateral occipital cortex	R
684	2.39	4.1	-58	-36	-10	middle temporal gyrus	L
Inanimate							
1934	6.75	-3.98	26	2	56	superior frontal gyrus	R
Frequency+							
760	4.11	4.11	-6	-68	30	precuneus	L (midline)
Frequency-							
1774	5.88	-4.59	-44	8	24	inferior frontal gyrus	L
484	1.38	-4.50	-44	-62	-8	inferior temporal gyrus	L
Remembered > Forgotten							
6713	18.50	6.47	-46	14	26	inferior frontal gyrus	L
826	3.11	4.51	-52	-48	-12	inferior temporal gyrus	L
707	4.09	4.09	-42	-68	26	lateral occipital cortex	L
Forgotten > Remembered							
1181	4.69	4.69	56	-38	32	supramarginal gyrus	R
965	3.53	3.53	-8	-70	38	precuneus	L
Stroop: Incongruent> Congruent							
4389	12.6	5.00	-42	24	18	inferior frontal gyrus	L
1891	6.38	4.79	46	22	24	middle frontal gyrus	R
1645	5.63	4.57	-30	-66	50	lateral occipital cortex	L
1639	5.61	4.74	0	16	54	superior frontal gyrus	L (midline)

Supplementary Table 5: Coordinates for all Alzheimer biomarker effects. Cortical labels come from the Harvard-Oxford atlas.

# Voxels	-log(p)	Max Z	x	y	z	LABEL	Hemisphere
Animacy $ptau_{181}$							
4230	13.00	4.82	38	12	28	middle frontal gyrus	R
1525	5.63	4.72	48	-32	-6	middle temporal gyrus	R
786	3.93	3.93	46	-12	50	precentral gyrus	R
602	3.67	3.67	-46	12	10	inferior frontal gyrus	L
Animacy tau							
720	2.65	4.11	48	-30	-8	middle temporal gyrus	R
Stroop $ptau_{181}$							
435	1.34	3.97	32	12	28	middle frontal gyrus	R
Stroop tau							
729	2.66	3.49	20	-10	20	caudate	R
High > Forgotten tau							
644	2.36	-3.83	2	4	52	supplementary motor cortex	R (midline)
431	1.35	-3.76	-24	-4	54	superior frontal gyrus	L